



## Radiological evidence of purulent infections in ancient Egyptian child mummies

Stephanie Panzer<sup>a,b,\*</sup>, Marcus Treitl<sup>a</sup>, Stephanie Zesch<sup>c</sup>, Wilfried Rosendahl<sup>c</sup>,  
Jana Helmbold-Doyé<sup>d</sup>, Randall C. Thompson<sup>e</sup>, Albert R. Zink<sup>f</sup>

<sup>a</sup> Department of Radiology, Berufsgenossenschaftliche Unfallklinik Murnau, Prof-Küntscher-Straße 8, D-82418 Murnau, Germany

<sup>b</sup> Institute of Biomechanics, Berufsgenossenschaftliche Unfallklinik Murnau and Paracelsus Medical University, Salzburg, Austria, Prof-Küntscher-Straße 8, D-82418 Murnau, Germany

<sup>c</sup> German Mummy Project, Reiss-Engelhorn-Museen, Museum Weltkulturen D5, D-68159 Mannheim, Germany

<sup>d</sup> Ägyptisches Museum und Papyrussammlung, Staatliche Museen zu Berlin, Geschwister-Scholl-Str. 6, D-10117 Berlin, Germany

<sup>e</sup> Saint Luke's Mid America Heart Institute, University of Missouri-Kansas City, 4330 Wornall Road, Kansas City, MO 64111, USA

<sup>f</sup> Institute for Mummy Studies, Eurac Research, Viale Druso 1, I-39100 Bolzano, Italy

### ARTICLE INFO

#### Keywords:

Multidetector computed tomography  
Abscess  
Infectious disease  
Paleoradiology  
Paleopathology  
Ancient Egyptian medicine

### ABSTRACT

**Objective:** To identify computed tomography (CT) findings of purulent infections in ancient Egyptian child mummies.

**Materials:** Whole-body CT examination of 21 ancient Egyptian child mummies from German (n = 18), Italian (n = 1), and Swiss museums (n = 2).

**Methods:** CT examinations were evaluated for estimation of age at death and sex of the children. CT examinations were systematically assessed for any CT findings of purulent infection.

**Results:** The estimated age at death of the children ranged from about one year to the age of 12–14 years (mean 4.8 years). Twelve children were assessed as male, seven as female and in two sex was indeterminate. Three out of 21 child mummies (14.3%) had radiological evidence of purulent infections. In one mummy, a bandage-like structure at the right lower leg was detected that most likely represented a dressing of a skin lesion.

**Conclusions:** This study appears to be the first to describe radiologically visualized structures consistent with dried pus in ancient Egyptian mummies. This study also appears to be the first to physically demonstrate an original ancient Egyptian dressing.

**Significance:** These cases may serve as models for further paleopathological investigation. The evidence of an original dressing contributes to our knowledge of ancient Egyptian medicine.

**Limitations:** CT was used as the only examination method as sampling of the wrapped mummies was not possible.

**Suggestions for further research:** Radiological-pathological correlation in mummies in which physical sampling is available may reveal further insights into purulent infections in ancient Egypt.

### 1. Introduction

In ancient Egypt, infections were likely a common aspect of daily life and the major cause of death (Thompson et al., 2013; Nunn, 2002). However, the overall evidence of infections in ancient mummies is limited, especially in the less frequently investigated child mummies. Infancy and childhood have long been recognized as critical periods of increased physiological stress, morbidity and mortality (Wheeler, 2012).

Childhood morbidity is also associated with reduced life expectancy in ancient populations (Wheeler, 2012; Finch, 2012; Crimmins and Finch, 2006).

Computed tomography (CT) has developed into the “gold-standard” of non-destructive imaging methods in human mummy studies (Panzer et al., 2019; Panzer et al., 2015; Panzer et al., 2013; Villa et al., 2015) including children (Oras et al., 2020; Villa et al., 2015; Davey et al., 2014). However, CT does not usually demonstrate results of infections,

\* Correspondence to: Department of Radiology, Trauma Center Murnau, Prof-Küntscher-Strasse 8, D-82418 Murnau, Germany.

E-mail addresses: [stephanie.panzer@bgu-murnau.de](mailto:stephanie.panzer@bgu-murnau.de) (S. Panzer), [marcus.treitl@bgu-murnau.de](mailto:marcus.treitl@bgu-murnau.de) (M. Treitl), [stephanie.zesch@mannheim.de](mailto:stephanie.zesch@mannheim.de) (S. Zesch), [wilfried.rosendahl@mannheim.de](mailto:wilfried.rosendahl@mannheim.de) (W. Rosendahl), [J.Helmbold-Doye@smb.spk-berlin.de](mailto:J.Helmbold-Doye@smb.spk-berlin.de) (J. Helmbold-Doyé), [rthompson@saint-lukes.org](mailto:rthompson@saint-lukes.org) (R.C. Thompson), [albert.zink@eurac.edu](mailto:albert.zink@eurac.edu) (A.R. Zink).

<https://doi.org/10.1016/j.ijpp.2021.12.002>

Received 30 August 2021; Received in revised form 26 November 2021; Accepted 19 December 2021

Available online 30 December 2021

1879-9817/© 2021 Elsevier Inc. All rights reserved.

particularly of soft tissue structures such as abscesses, although these must have been a common occurrence. Regarding bacterial infections, molecular evidence of bacteremia has, however, been reported in an ancient Egyptian infant mummy (Zink et al., 2000).

In this study, whole-body CT examinations of 21 ancient Egyptian child mummies were systematically assessed for any CT finding of purulent infection.

## 2. Materials and methods

### 2.1. Materials

In this study, we investigated 21 externally well preserved ancient Egyptian child mummies from German (n = 18), Italian (n = 1), and Swiss museums (n = 2). The bodies of all children were artificially mummified. The chronology of the mummies was determined based on 14C dating and museum records.

### 2.2. Methods

Whole-body CT examinations were performed at the respective museum locations with a range of scanning parameters based upon the available CT scanner (slice thickness 0.6–1.5 mm, 110–140 kV).

Age at death was estimated from dental (Ubelaker, 1978; Moorrees et al., 1963a, 1963b) and skeletal development (Boccone et al., 2010; Scheuer and Black, 2000; Stloukal and Hanáková, 1978). Sex was assessed through the identification of genitalia, iconography of mummy decoration, and/or the name written on the outermost textiles on a related coffin or papyrus.

CT scans were systematically reviewed for structures most likely representing dried pus by the first author. Based on clinical radiological and paleoradiological experience, a list of anatomical regions of common sites of infections was used for standardized assessment and documentation. These regions included the soft tissues of the paranasal sinuses, the soft tissues of the neck, the soft tissues of the spinal column, the upper extremity (shoulder, upper arm, elbow, forearm, wrist, hand), and the lower extremity (hip, thigh, knee, lower leg, ankle, foot). The interpretation of CT findings followed clinical radiological criteria taking into account any changes of CT appearance due to taphonomy. Specifically, asymmetry was a major focus of the radiologic inspection. If additional structures were seen, changes of taphonomy were considered likely when there were anatomic correlates of manipulation or foreign bodies including resin that would account for the asymmetry. Also, if destruction of structures was seen, the relevant images were carefully reviewed for signs of manipulation / artificial mummification that could account for the destruction. After changes of taphonomy were excluded in this way, pathomechanisms for the conspicuous findings were considered before attributing them to disease processes. Conspicuous findings of purulent infections were reviewed and interpreted by consensus between the first author and one co-author.

## 3. Results

The mummies predominantly dated to the Ptolemaic Period (332–30 BCE) and Roman Period (30 BCE–395 CE) (according to Shaw (2003)). The estimated age at death of the children ranged from about one year to the age of 12–14 years (mean 4.8 years). Twelve children were assessed as male, seven as female and in two, sex was indeterminate.

Three out of the 21 child mummies (14.3%) had radiological evidence of purulent infections:

### 3.1. Case 1

In the mummy of a nine to eleven-year-old boy (Ptolemaic–Roman Period), CT indicated purulent sinusitis as evidenced by dried masses, especially in the basal parts of both maxillary sinuses (Hounsfield Unit

(HU) ca. 158) (Fig. 1a and b). The frontal skull base was intact, so that there was no evidence for artificial removal of the brain. The ethmoid sinus, the nasal septum and the medial margins of both maxillary sinuses were intact, and the nasal passage was ventilated and free from any masses or substances, and thus were without indicators of artificial manipulation in the region of the nasal cavity. Additionally, the CT images demonstrated severe peritonsillar and/or parapharyngeal abscess with rupture into the pharyngeal space, evident by remnants of suggested dried pus within the postinfectious soft tissue defect (HU ca. 58) and the oral (HU ca. 186) and pharyngeal cavity (HU ca.161) (Fig. 1). The pharyngeal wall and adjacent soft tissues, including the jugular vein and carotid artery, were well preserved allowing for detailed diagnosis (Harnsberger et al., 2004). In the advanced stage of infection, as shown in the child mummy, it was not possible to differentiate between a peritonsillar or parapharyngeal abscess with the complication of additional necrotizing fasciitis (Klug, 2017). No substances with similar densities to those suggested as pus were found externally around the nose or mouth, and there was no evidence of artificial mummification using resins in this mummy.

### 3.2. Case 2

In the mummy of a two and a half to four-year-old girl (1st–2nd century CE), a bandage-like structure at the left lower leg was visible that most likely represents a dressing of a skin lesion. As the mummy was completely wrapped by thick layers of textile, the bandage is believed to be original. It had a size of 20 × 12 × 9 mm and densities of ca. -2 HU within the central portion and 128 HU in the peripheral parts. This structure overlies masses within the adjacent soft tissues, which are consistent with dried pus, thus indicating the individual had purulent cellulitis or abscess (HU ca. -54) (Raff and Kroshinsky, 2016; Resnick, 2002) (Fig. 2). Overall, there was no evidence of artificial mummification by means of resins.

### 3.3. Case 3

In the mummy of a two to three-year-old boy (1st–2nd century CE), a dried fluid level was found in the enlarged capsule of the right hip (HU ca. 187) (Fig. 3), most probably indicating dried pus in septic arthritis (Resnick, 2002). The location in the ventral part of the joint could be explained by sedimentation of the solid parts of the suspension during prone position of the body within the mummification procedure. Due to the extent at this level, an underlying hematoma was unlikely. No defects of the adjacent soft tissues were detectable, and no similar structures were found external to the right hip.

## 4. Discussion

In this study, modern CT imaging with high spatial resolution, systematic assessment of soft tissues, and authors' experience in paleoradiology and taphonomy led to the recognition of purulent infections in three out of 21 ancient Egyptian child mummies. All three mummies had very good soft tissue preservation.

The authors did not find any comparable case of infection of paranasal sinuses in the paleopathological literature of ancient Egypt. However, osseous changes of the margins of the maxillary sinus indicating chronic disease have been found in adult mummies (Marquez et al., 2015). Also, the authors did not find any comparable case of purulent infections, such as peri-/retropharyngeal abscess, septic arthritis and purulent cellulitis or soft tissues abscesses in the literature on ancient Egyptian mummies. Tonsillar-peritonsillar abscess is reported as the most common deep neck infection in children and young adults in the clinical literature (Harnsberger et al., 2004). Cellulitis and abscesses are a common global health burden in the modern world (Raff and Kroshinsky, 2016). Purulent infections must have certainly occurred in ancient Egypt (Nunn, 2002). In the pre-antibiotic era, many infections

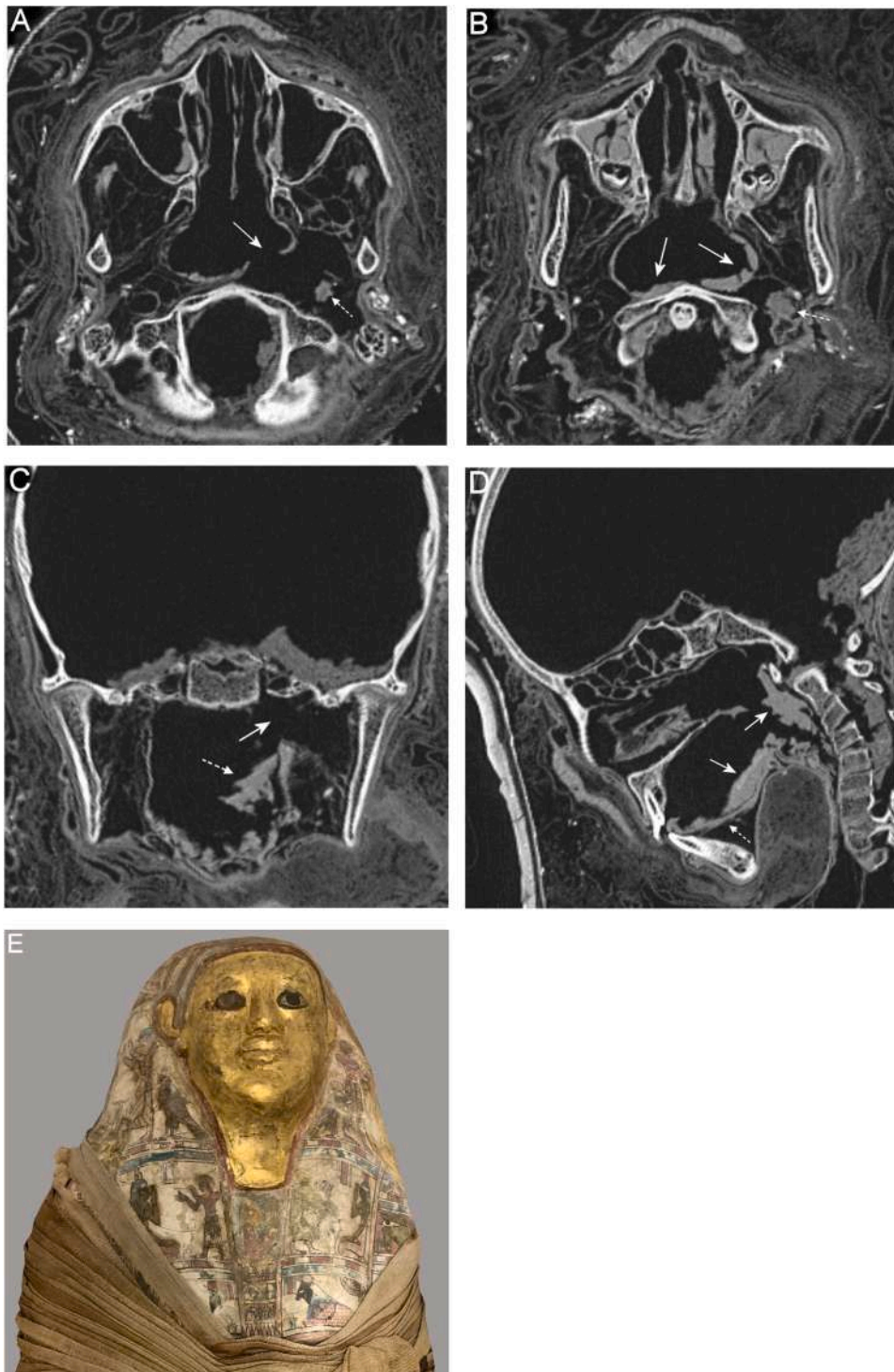


**Fig. 1.** CT findings of purulent sinusitis and peritonsillar and/or parapharyngeal abscess. (A) Axial multiplanar reconstruction (MPR) demonstrates a broad defect of the thickened pharyngeal wall on the left side (solid arrow). The soft tissues of the parapharyngeal space on the left side, including the carotid space, are severely disrupted extending to the ventral occipital bone, the mastoid, and the masticator space. This defect was interpreted to be the result of inflamed and/or necrotic tissues and fluids that decayed to a great extent during the mummification process and became replaced by air. Within this area, a small irregular mass is detectable (dotted arrow), most likely a remnant of pus. Note the band-shaped dried masses adjacent to the margins of both maxillary sinuses. (B) Axial MPR below illustrates another mass within the area of destroyed soft tissues (dotted arrow) as well as masses located along the posterior pharyngeal wall (solid arrows). Both maxillary sinuses are filled with dried masses with tears in their basal portions (asterisks) that are likely remnants of dried pus. (C) Coronal MPR shows the defect of the pharyngeal wall (arrow) and the adjacent soft tissue destruction as well as dried masses within the oral cavity (dotted arrow). (D) Sagittal MPR illustrates the masses (solid arrows) along the posterior pharyngeal wall and on the preserved tongue (dotted arrow). Note preservation of brain in the dorsal fossa and of the cervical spinal cord. (E) Photograph of the upper part of the mummy that was wrapped with linen bandages in a rhomboid pattern; provenance unknown. The head and shoulders were covered with a partially gilded cartonnage mask that was decorated with religious scenes depicting the deceased, gods and goddesses and symbols referring to the ancient Egyptian afterlife concept (©Senckenberg) (inventory number Ä 15 (IN 2462a), Senckenberg Forschungsinstitut und Naturmuseum, Frankfurt a. M., Germany).

would have led to severe illness with bacteremia and subsequent systemic pathology. Septicemia was considered as the likely cause of death in the child mummies with purulent infections in this study.

Hounsfield Units (HU) express the X-ray attenuation coefficients of each voxel on CT images. Air is calibrated to -1000 HU and water to 0 HU (Kalender, 2006). Villa and Lynnerup have reported HU ranges of various tissues in Egyptian mummies. Muscles, for example, had a mean HU of -122 with a range of -716 (10th percentile) to 136 (90th percentile). In contrast, contemporary forensic cases demonstrated a mean HU of 48 with a range of 28 (10th percentile) to 62 (90th percentile) in muscle (Villa and Lynnerup, 2012), similar to the HU

values of living patients. Mummification processes preserve tissues from postmortem decay. These effects and processes are described by the term “taphonomy” (Aufderheide, 2003). As these diverse processes change the tissues from their original state, their densities and HU also change. HU of structures believed to be pus in this study varied between -54 in Case 2, 58–186 in Case 1, and 187 in Case 3. In Case 1, HU of what is believed to be dried pus in the paranasal sinuses and the suggested pus within the oral cavity had comparable HU. This indicates that similar structures underwent similar taphonomic changes within this one body during mummification. The HU values of pus in Case 1 and Case 3 were also similar. Gostner et al. (2013) have provided a list of HU of foreign



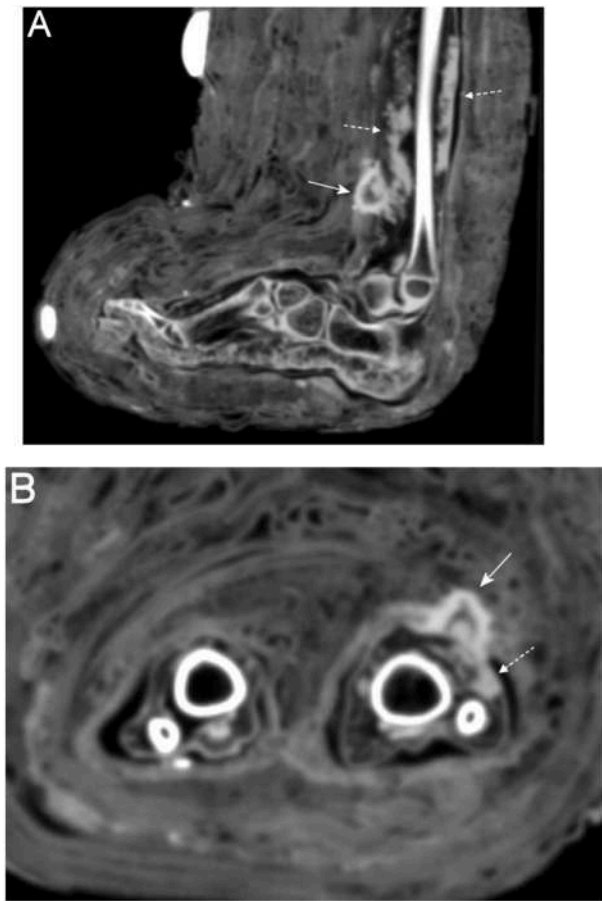


**Fig. 2.** CT findings of soft tissue infection in the lower leg. (A) Sagittal and (B) axial MPRs of the lower legs depict a conical foreign body at the surface of the left lower leg (solid arrow) most likely representing a dressing over a skin lesion. Below the bandage, confluent hyperdense masses expand within the adjacent soft tissue posteriorly and to the left, consistent with dried pus (dotted arrows). The left lower leg is markedly swollen. Shrunken remnants of muscles are visible on both sides dorsal to the tibia. (C) Photograph of the mummy from the so-called “Tomb of Aline”, Hawara (Fayoum Oasis). The outermost textile layers were created by cross-folded linen bandages in a rhomboid pattern, decorated with several painted and gilded stucco buttons. A portrait of the infant was painted on linen fabric and placed across the facial region (©SMB, Ägyptisches Museum und Papyrussammlung, Foto: Sandra Steiß) (inventory number ÄM 11412, Ägyptisches Museum und Papyrussammlung, Berlin, Germany).

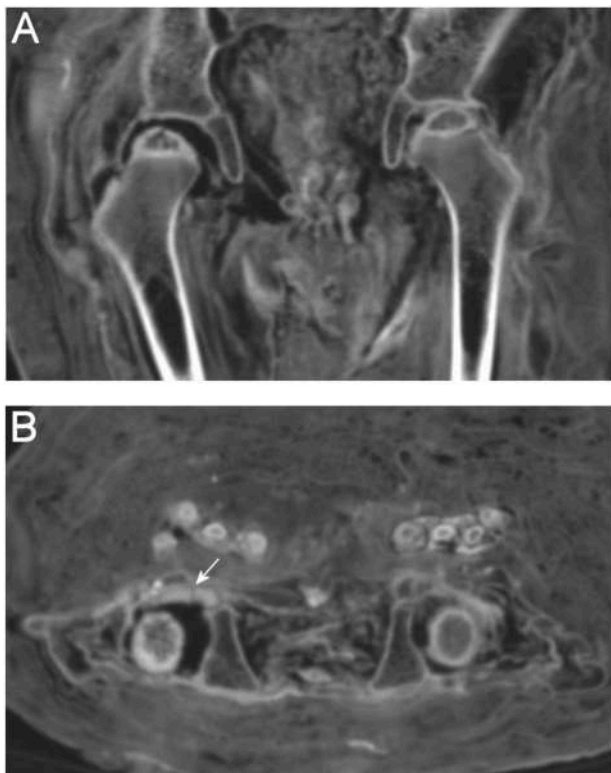


**Fig. 3.** CT findings of septic hip arthritis. (A) Coronal MPR demonstrates a widened joint capsule of the right hip most probably caused by a large joint effusion in the lifetime of the boy that resolved and was replaced by air during the mummification process. (B) Axial MPR depicts a dried fluid level in the ventral part of the right hip joint (arrow) that most likely represents dried pus. (C) Photograph of the mummy. This portrait mummy is from the same tomb as the mummy in Fig. 2, showing a similar style of mummy decoration (©SMB, Ägyptisches Museum und Papyrussammlung, Foto: Sandra Steiß) (inventory number ÄM 11413, Ägyptisches Museum und Papyrussammlung, Berlin, Germany).

objects in ancient and historic mummies. HU for resin is given as 71 with a standard deviation of 23.7. Thus, HU of masses that are believed to be dried pus were clearly lower than those for resin in Case 1, clearly higher in Case 3 and predominantly higher in Case 2.

From this study, the following conclusions can be drawn for radiological assessment of purulent infections in ancient Egyptian mummies:

- Radiologists should be aware of advanced stages of infectious diseases as shown on these CT images from ancient pre-antibiotic times.
- Identification and interpretation of asymmetry is one major tool to aid in making these diagnoses.
- There exist no specific reference values for HU density of human mummified tissues and intracorporal fluids.

This study appears to be the first to physically note an original ancient Egyptian dressing. Such treatment was reported in the Edwin Smith Papyrus, a medical text and trauma treatise from ancient Egypt (ca. 1650–1550 BCE). Case 41 describes an infection of a wound: “One who has infection in a wound in his chest, which is inflamed-hot/infected and because of which he is febrile”. The wound is described as remaining open, greatly inflamed and swollen, hot, red, and with an oily discharge. This description demonstrates the ancient Egyptians’ recognition of three of the four cardinal signs of inflammation, defined later by Celsus (ca. 25 BCE–50 CE) as “tumor, rubor, calor, dolor” (Sanchez and Meltzer, 2012; Celsus). The ancient Egyptian physician recommended “cooling remedies for drawing out the heat from the mouth of the wound”, “a remedy for drying the wound” including natron salt, and a powder, all of them applied with a bandage of the wound. “If the same occurs in any body part” the physician recommended to “treat it according to these instructions” (Sanchez and Meltzer, 2012). The relatively dense appearance of the suggested dressing could be the result of natron content. Measurements of natron revealed HU up to 800 (Notman and Aufderheide, 1992).

The main limitation of this study is that CT was used as the only examination method for diagnosis of purulent infections. Sampling of the mummies was not available for radiological-pathological correlation. In addition to the important issue of ethical approaches to human remains (Squires et al., 2020; Moissidou et al., 2015), sampling would have partially destroyed the extensive and elaborate wrapping of the investigated museum mummies.

## 5. Conclusions

This study appears to be the first to describe radiologically visualized structures consistent with dried pus in ancient Egyptian mummies. As a result, these cases may serve as models for further paleopathological investigation. The evidence of an original dressing contributes to our knowledge of ancient Egyptian medicine.

## Acknowledgments

We are very grateful to the directors and curators of the museums for sharing the CT data sets and supporting us with background information on the mummies: Gerhard Hotz (Naturhistorisches Museum Basel, Basel), André Wiese (Antikenmuseum Basel und Sammlung Ludwig, Basel), Friederike Seyfried (Ägyptisches Museum und Papyrussammlung, Berlin), Dietrich Raue (Ägyptisches Museum - Georg Steindorff – der Universität Leipzig, Leipzig), Regine Schulz and Oliver Gauert (Roemer- und Pelizaeus-Museum, Hildesheim), Friedemann Schrenk (Senckenberg Forschungsinstitut und Naturmuseum, Frankfurt a. M.), Christian Greco (Museo Egizio, Turin). We acknowledge the support of the HORUS study team for the acquisition of the CT scans at the museums of Berlin and Torino.

## References

- Aufderheide, A.C., 2003. *The Scientific Study of Mummies*. Cambridge University Press, Cambridge.
- Celsus, A.C. De Medicina. (<http://penelope.uchicago.edu/Thayer/E/Roman/Texts/Celsus/home.html>). (Assessed 18 April 2021).
- Boccone, S., Cremasco, M.M., Bartoluzzi, S., Moggi-Cecchi, J., Massa, E.R., 2010. Age estimation in subadult Egyptian remains. *Homo* 61, 337–358.
- Crimmins, E.M., Finch, C.E., 2006. Infection, inflammation, height, and longevity. *Proc. Natl. Acad. Sci. USA* 103 (2), 498–503.
- Davey, J., Taylor, J.H., Drummer, O.H., 2014. The utilisation of modern forensic imaging in the investigation of graeco-roman child mummies. *J. Egypt. Archaeol.* 100 (1), 195–208.
- Finch, C.E., 2012. Evolution of the human lifespan, past, present, and future: phases in the evolution of human life expectancy in relation to the inflammatory load. *Proc. Am. Philos. Soc.* 156 (1), 9–44.
- Gostner, P., Bonelli, M., Pernter, P., Graefen, A., Zink, A., 2013. New radiological approach for analysis and identification of foreign objects in ancient and historic mummies. *J. Archaeol. Sci.* 40 (2), 1003–1011.
- Harnsberger, H.R., Hudgins, P.A., Davidson, H.C., Wiggins III, R.H., 2004. *Head & Neck, first ed.* Amirsys, Salt Lake City. pp. III 1 6–9.
- Kalender, W.A., 2006. *Computertomographie. Grundlagen, Gerätetechnologie, Bildqualität, Anwendungen*, second ed. Publicis Corporate Publishing, Erlangen.
- Klug, T.E., 2017. Peritonsillar abscess: clinical aspects of microbiology, risk factors, and the association with parapharyngeal abscess. *Dan. Med. J.* 64 (3), B5333.
- Márquez, S., Lawson, W., Mowbray, K., Delman, B.N., Laitman, J.T., 2015. CT examination of nose and paranasal sinuses of egyptian mummies and three distinct human population groups: anthropological and clinical implications. *Anat. Rec.* 298 (6), 1072–1084.
- Moissidou, D., Day, J., Shin, D.H., Bianucci, R., 2015. Invasive versus non invasive methods applied to mummy research: will this controversy ever be solved? *BioMed Res. Int.*, 192829.
- Moorrees, C.F.A., Fanning, E.A., Hunt Jr., E.E., 1963a. Age variation of formation stages for ten permanent teeth. *J. Dent. Res.* 42 (6), 1490–1502.
- Moorrees, C.F.A., Fanning, E.A., Hunt Jr., E.E., 1963b. Formation and resorption of three deciduous teeth in children. *Am. J. Phys. Anthropol.* 21 (2), 205–213.
- Notman, D.N.H., Aufderheide, A.C., 1992. Experimental mummification and computed imaging. In: *Proceedings of the First World Congress on Mummy Studies*. Archaeological and Ethnographical Museum of Tenerife, Santa Cruz, Tenerife, Canary Islands. pp. 821–828.
- Nunn, J.F., 2002. In: Nunn, J.F. (Ed.), *Ancient Egyptian Medicine*. University of Oklahoma Press, pp. 59–60.
- Oras, E., Anderson, J., Törv, M., Vahur, S., Ramm, R., Remmer, S., Mölder, M., Malve, M., Saag, L., Saage, R., Teearu-Ojakäär, A., Peets, P., Tambets, K., Metspalu, M., Lees, D.C., Barclay, M., Hall, M., Ikram, S., Piombino-Mascali, D., 2020. Multidisciplinary investigation of two Egyptian child mummies curated at the University of Tartu Art Museum, Estonia (Late/Graeco-Roman Periods). *PLoS One* 15 (1), e0227446.
- Panzer, S., Borumandi, F., Wanek, J., Papageorgopoulou, C., Shved, N., Colacicco, G., Rühli, F.J., 2013. Modeling ancient Egyptian embalming: radiological assessment of experimentally mummified human tissue by CT and MRI. *Skelet. Radiol.* 42 (11), 1527–1535.
- Panzer, S., Ketterl, S., Bicker, R., Schoske, S., Nerlich, A.G., 2019. How to CT scan human mummies: theoretical considerations and examples of use. *Int. J. Paleopathol.* 26, 122–134.
- Panzer, S., Mc Coy, M.R., Hitzl, W., Piombino-Mascali, D., Jankauskas, R., Zink, A.R., Augat, P., 2015. Checklist and scoring system for the assessment of soft tissue preservation in CT examinations of human mummies. *PLoS One* 10, e0133364.
- Raff, A.B., Kroshinsky, D., 2016. Cellulitis: a review. *JAMA* 316 (3), 325–337.
- Resnick, D., 2002. *Diagnosis of Bone and Joint Disorders*, fourth ed. W.B. Saunders Company, Philadelphia, pp. 2378–2469.
- Sanchez, G.M., Meltzer, E.S., 2012. *The Edwin Smith Papyrus. Updated Translation of the Trauma Treatise and Modern Medical Commentaries*. Lockwood Press, pp. 250–257.
- Scheuer, L., Black, S., 2000. *Developmental Juvenile Osteology*. Academic Press, London.
- Shaw, I., 2003. In: Shaw, I. (Ed.), *The Oxford History of Ancient Egypt*. Oxford University Press, pp. 479–483.
- Squires, K., Booth, T., Roberts, C.A., 2020. The ethics of sampling human skeletal remains for destructive analyses. In: Squires, K., Erickson, D., Márquez-Grant, N. (Eds.), *Ethical Approaches to Human Remains. A Global Challenge in Bioarchaeology and Forensic Anthropology*. Springer Nature Switzerland, Cham, pp. 265–298.
- Stloukal, M., Hanáková, H., 1978. Die Länge der Längsknochen altslawischer Bevölkerungen – Unter besonderer Berücksichtigung von Wachstumsfragen. *Homo* 29, 53–69.
- Thompson, R.C., Allam, A.H., Lombardi, G.P., Wann, L.S., Sutherland, M.L., Sutherland, J.D., Soliman, M.A., Frohlich, B., Mininberg, D.T., Monge, J.M., Vallodolid, C.M., Cox, S.L., Abd el-Maksoud, G., Badr, I., Miyamoto, M.I., el-Halim Nur el-Din, A., Narula, J., Finch, C.E., Thomas, G.S., 2013. Atherosclerosis across 4000 years of human history: the Horus study of four ancient populations. *Lancet* 381 (9873), 1211–1222.
- Ubelaker, D.H., 1978. *Human Skeletal Remains: Excavation, Analysis and Interpretation*. Smithsonian Institution Press, Washington, DC.
- Villa, C., Davey, J., Craig, P.J., Drummer, O.H., Lynnerup, N., 2015. The advantage of CT scans and 3D visualizations in the analysis of three child mummies from the Graeco-Roman Period. *Anthropol. Anz.* 72 (1), 55–65.

Villa, C., Lynnerup, N., 2012. Hounsfield units ranges in CT-scans of bog bodies and mummies. *Anthropol. Anz.: Bericht über biol.-anthropol. Lit.* 69 (2), 127–145.

Wheeler, S.M., 2012. Nutritional and disease stress of juveniles from the Dakhleh Oasis, Egypt. *Int. J. Osteoarchaeol.* 22 (2), 219–234.

Zink, A., Reischl, U., Wolf, H., Nerlich, A.G., 2000. Molecular evidence of bacteremia by gastrointestinal pathogenic bacteria in an infant mummy from ancient Egypt. *Arch. Pathol. Lab. Med.* 124 (11), 1614–1618.